ANZIAM J. **63** (2021), 203–227
doi:10.1017/S1446181121000237

LOCALIZED RADIAL BASIS FUNCTIONS FOR NO-ARBITRAGE PRICING OF OPTIONS UNDER STOCHASTIC ALPHA–BETA–RHO DYNAMICS

N. THAKOOR [1]

(Received 29 April, 2020; accepted 7 April, 2021; first published online 19 August, 2021)

Abstract

Closed-form explicit formulas for implied Black–Scholes volatilities provide a rapid evaluation method for European options under the popular stochastic alpha–beta–rho (SABR) model. However, it is well known that computed prices using the implied volatilities are only accurate for short-term maturities, but, for longer maturities, a more accurate method is required. This work addresses this accuracy problem for long-term maturities by numerically solving the no-arbitrage partial differential equation with an absorbing boundary condition at zero. Localized radial basis functions in a finite-difference mode are employed for the development of a computational method for solving the resulting two-dimensional pricing equation. The proposed method can use either multiquadrics or inverse multiquadrics, which are shown to have comparable performances. Numerical results illustrate the accuracy of the proposed method and, more importantly, that the computed risk-neutral probability densities are nonnegative. These two key properties indicate that the method of solution using localized meshless methods is a viable and efficient means for price computations under SABR dynamics.

2020 *Mathematics subject classification*: primary 65M06; secondary 91G20.

Keywords and phrases: stochastic alpha–beta–rho model, local radial basis functions, financial options, no-arbitrage prices.

1. Introduction

An implied volatility is the value of the volatility parameter for which an observed market price fits the Black–Scholes option pricing formula [3]. Maturity and strike-dependent computed implied volatilities, contrary to the assumption of constant volatility in the Black–Scholes model, resulted in the search for models capable of fitting market-observed volatilities. Dupire [11] introduced a local volatility model, where, for a given maturity, the asset price process matches the strike-dependent

[1]Department of Mathematics, University of Mauritius, Reduit 80837, Mauritius;
e-mail: n.thakoor@uom.ac.mu
© Australian Mathematical Society 2021

https://doi.org/10.1017/S1446181121000237 Published online by Cambridge University Press

volatility profile, usually referred to as a smile dynamics. One drawback of the Dupire model is that the smile shifts are opposite to the observed market behaviour of asset prices. This observation led to the introduction of the stochastic alpha–beta–rho (SABR) model [16]. The widespread use of SABR in financial markets stems from the facts that, in addition to being a local stochastic volatility model and having the capability of fitting various market volatility structures, this option pricing model also eliminates the problem of asset prices and smiles moving in opposite directions as in Dupire's model.

The SABR model incorporates a constant elasticity of variance (CEV)-type diffusion process for the forward price whose volatility follows a Black–Scholes-type diffusion with zero drift. The probability of the forward price process hitting zero is positive, but it exponentially decays to zero with shrinking time horizon with faster convergence rates for large initial asset prices or elasticity parameter of the CEV dynamics in the model or small values of the forward price's initial volatility or the volatility of its volatility process [6].

Computations of prices which are arbitrage-free require the imposition of an absorbing boundary condition at zero. Ignoring this boundary condition in a numerical method runs the risk of producing negative probability densities for low strikes [17]. The quantification of not having an absorbing boundary condition carried out by Chen and Yang [6] shows that the approximation error in prices is negligible only for small maturities.

Specifying an absorbing boundary condition at zero and using an expansion around a one-dimensional Bessel process, the closed-form approximation for European options [33] has been shown to be accurate for small maturity problems [31]. This implies that the search for a numerical method capable of accurately pricing options with large maturities needs to incorporate the absorbing boundary condition in order to ensure that computed prices are arbitrage-free.

Observing that the boundary layer next to zero forward price has a significant influence on pricing, an effective one-dimensional equation for the probability density with an absorbing boundary condition was derived [17]. By numerical solution of this equation using a Crank–Nicolson time-stepping scheme [8], call and put values can be obtained by numerical integration and this procedure leads to arbitrage-free prices. Other methods proposed for the numerical determination of the probability density include the trapezoidal rule with the second-order backward difference formula [21] and an exponential time integration scheme [29]. This one-dimensional approach is not exact, and the solution of the two-dimensional SABR partial differential equation (PDE) provides a more accurate means for price determination.

This work addresses the issue of accurate price computations by proposing a localized radial basis functions (RBFs) method for solving the two-dimensional SABR pricing equation. Applications of RBFs in a local mode have gained much importance in the numerical solutions of PDEs in the field of computational fluid dynamics. Their applications to PDEs in finance have been much less considered, and the present work develops a new local RBF method for the solution of the arbitrage-free SABR PDE.

https://doi.org/10.1017/S1446181121000237 Published online by Cambridge University Press

Weighting coefficients for generalized multiquadrics (GMQ) presented here are new. The numerical discretization in space is then carried out using multiquadrics and inverse multiquadrics, which are special cases of GMQ. One clear advantage of using RBFs is that due to their meshless nature, unstructured grids or randomly scattered grid points can be employed to achieve accurate prices. An extensive set of numerical examples using structured and randomly scattered points are considered to demonstrate that accurate no-arbitrage prices are computed.

The presentation of the work carried out is as follows. The SABR PDE is described in Section 2 and a brief account of some recent studies related to the SABR model is mentioned. Local generalized multiquadrics approximations for the first and second derivatives are derived in Section 3. The numerical method for the valuation of options under SABR is developed in Section 4 and the time-stepping scheme for the solution of the system of differential equations is described. Numerical examples are considered in Section 5 and a summary of the work, conclusions reached and possible future work are given in Section 6.

2. No-arbitrage SABR PDE

Consider a financial market with a risky asset with forward price process F_t and volatility α_t over a time horizon $0 \le t \le T$. Let W_t and $\widehat{W}_t$ be Brownian motions on the filtered probability space $(\Omega, \mathcal{F}, \mathcal{F}_t, \mathbb{Q})$, where Ω is the sample space, $\mathcal{F}$ is a σ-algebra and $\mathbb{Q}$ is a martingale measure. The filtration $\mathcal{F}_t$ is defined below. Let $\rho \in (-1, 1)$ be the correlation parameter between the Brownian motion W_t driving the constant elasticity of variance dynamics with elasticity parameter β for F_t and the Brownian motion $\widehat{W}_t$ driving the geometric Brownian motion process with zero drift for α_t [16]. Let

$$\overline{W}_t = (1-\rho^2)^{-1/2}(W_t - \rho\widehat{W}_t).$$

Consider the filtration $\mathcal{F}_t = \mathcal{F}_t^{\overline{W}} \otimes \mathcal{F}_t^{\widehat{W}}$, where $\mathcal{F}_t^{\overline{W}}$ and $\mathcal{F}_t^{\widehat{W}}$ are the filtrations generated by the independent Brownian motions $\overline{W}_t$ and $\widehat{W}_t$, respectively. Denoting by ν the volatility of the volatility process α_t, the SABR dynamics of (F_t, α_t) can be specified by the system of two stochastic differential equations given by

$$\begin{aligned} dF_t &= \alpha_t\Big(\sqrt{1-\rho^2}d\overline{W}_t + \rho d\widehat{W}_t\Big)F_t^{\beta}, \quad F_0 = f, \\ d\alpha_t &= \nu\alpha_t d\widehat{W}_t, \quad \alpha_0 = \hat{\alpha}. \end{aligned} \tag{2.1}$$

Let $\phi(F_t, \alpha_t)$ be the payoff at time t of a contingent claim on the underlying asset. The infinitesimal generator $\mathcal{L}$ of the payoff $\phi(F, \alpha)$ defined as

$$\mathcal{L}\phi(F,\alpha) = \lim_{t\to 0^+} \frac{\mathbb{E}[\phi(F_t,\alpha_t) \mid F_t = F, \alpha_t = \alpha] - \phi(F,\alpha)}{t}$$

https://doi.org/10.1017/S1446181121000237 Published online by Cambridge University Press

is given by Cui et al. [9] as

$$\mathcal{L}\phi = \frac{1}{2}\alpha^2 F^{2\beta}\frac{\partial^2\phi}{\partial F^2} + \rho\nu\alpha^2\frac{\partial^2\phi}{\partial F\partial\alpha} + \frac{1}{2}\nu^2\alpha^2\frac{\partial^2\phi}{\partial\alpha^2}.$$

The payoff for a call option with strike K is $\phi(F,\alpha) = (F-K)^+ = \max(F-K,0)$, and for a put option $\phi(F,\alpha) = (K-F)^+$. Let η_t be the first time that the forward price process hits zero, and let the time-t price of a contingent claim on the underlying asset be given by

$$V(F,\alpha,t) = \mathbb{E}[\phi(F_t,\alpha_t) \mid F_t = F, \alpha_t = \alpha].$$

Let the corresponding call price be $V_c(F,\alpha,t)$ and the put price be $V_p(F,\alpha,t)$. Then, denoting the indicator function for a set S by $\mathbf{1}_S$, the call and put prices are given by [33]

$$V_c(F,\alpha,t) = \mathbb{E}[(F_T-K)^+\mathbf{1}_{\{\eta_t>T\}} \mid F_t = f,\ \alpha_t = \alpha]$$

and

$$V_p(F,\alpha,t) = \mathbb{E}[(K-F_T)^+\mathbf{1}_{\{\eta_t>T\}} \mid F_t = f,\ \alpha_t = \alpha] + K\mathbb{E}[\mathbf{1}_{\{\eta_t\le T\}} \mid F_t = f,\ \alpha_t = \alpha].$$

Pricing a European call option with strike K is the same as pricing a down-and-out call option with a knockout boundary at zero. The call price $V_c(F,\alpha,t)$ is the unique solution [33] of the PDE given by

$$\frac{\partial V(F,\alpha,t)}{\partial t} + \mathcal{L}V(F,\alpha,t) = 0, \quad (F,\alpha,t) \in \mathbb{R}^+\times\mathbb{R}^+\times[0,T] \tag{2.2}$$

with terminal condition $V(F,\alpha,T) = (F-K)^+$ and boundary condition $V(0,\alpha,t) = 0$.

Pricing a European put option with strike K with an absorbing boundary condition at zero is the same as pricing a down-and-out put option with a rebate payment of K if the knock-out boundary at zero is reached. An analytical approximation for the probability that the forward price process hits zero was derived by Yang and Wan [35]. Let

$$\begin{aligned} P_0(F,\alpha,t) &= \mathbb{E}[\mathbf{1}_{\{\eta_t>T\}} \mid F_t = f,\ \alpha_t = \alpha] \\ &= \mathbb{P}(\eta_t > T \mid F_t = f,\ \alpha_t = \alpha). \end{aligned}$$

Then $P_0(F,\alpha,t)$ is the unique solution of the PDE

$$\frac{\partial P_0(F,\alpha,t)}{\partial t} + \mathcal{L}P_0(F,\alpha,t) = 0, \quad (F,\alpha,t) \in \mathbb{R}^+\times\mathbb{R}^+\times[0,T]$$

with condition $P_0(0,\alpha,t) = 0$ and boundary condition $P_0(F,\alpha,T) = 1$.

It then follows that the European put price is given by

$$V_p(F,\alpha,t) = P_1(F,\alpha,t) + K(1-P_0(F,\alpha,t)),$$

https://doi.org/10.1017/S1446181121000237 Published online by Cambridge University Press

where $P_1(F, \alpha, t)$ is the unique solution of the PDE

$$\frac{\partial P_1(F, \alpha, t)}{\partial t} + \mathcal{L}P_1(F, \alpha, t) = 0, \quad (F, \alpha, t) \in \mathbb{R}^+ \times \mathbb{R}^+ \times [0, T]$$

with terminal condition $P_1(F, \alpha, T) = (K - F)^+$ and boundary condition $P_1(0, \alpha, t) = 0$.

3. General multiquadrics finite-difference approximations

A numerical scheme for the solution of (2.2) requires approximations of the space derivatives $\partial^2 V/\partial F^2$, $\partial^2 V/\partial F \partial \alpha$ and $\partial^2 V/\partial \alpha^2$. The method proposed here is based on obtaining three-point finite-difference (FD) approximations of the derivatives using general multiquadrics (GMQ) radial basis functions.

Let $u(x)$ be a one-dimensional function whose derivatives $u'(x_0)$ and $u''(x_0)$ are to be approximated using values of u at the nodes $x_0 - h$, x_0 and $x_0 + h$. Thus, denoting by $u^{(k)}(x_0)$ the kth derivative of u at the node x_0, we seek approximations of the form

$$u^{(k)}(x) \approx a_{-1}^{(k)} u(x_0 - h) + a_0^{(k)} u(x_0) + a_1^{(k)} u(x_0 + h).$$

The weighting coefficients $\{a_i^{(k)}\}_{-1 \le i \le 1}^{k=1,2}$ are to be found using GMQs given by

$$\varphi_i(x) = (c^2 + (x - x_0 - ih)^2)^{m/2}, \quad -1 \le i \le 1, \tag{3.1}$$

such that

$$\varphi_i^{(k)}(x_0) = a_{-1}^{(k)} \varphi_i(x_0 - h) + a_0^{(k)} \varphi_i(x_0) + a_1^{(k)} \varphi_i(x_0 + h), \quad -1 \le i \le 1.$$

Note that

$$\varphi_i'(x) = \frac{m(x - x_0 - ih)\varphi_i(x)}{c^2 + (x - x_0 - ih)^2}, \quad \varphi_i''(x) = \frac{m(c^2 + (m-1)(x - x_0 - ih)^2)\varphi_i(x)}{(c^2 + (x - x_0 - ih)^2)^2}.$$

Letting

$$q_0 = \frac{mh(c^2 + h^2)^{m/2}}{c^2 + h^2}, \quad w_j = (c^2 + j^2 h^2)^{m/2}, \quad 0 \le j \le 2,$$

the weighting coefficients for the approximation of the first derivative then satisfy the equation

$$\begin{pmatrix} w_0 & w_1 & w_2 \\ w_1 & w_0 & w_1 \\ w_2 & w_1 & w_0 \end{pmatrix} \begin{pmatrix} a_{-1}^{(1)} \\ a_0^{(1)} \\ a_1^{(1)} \end{pmatrix} = q_0 \begin{pmatrix} 1 \\ 0 \\ -1 \end{pmatrix}.$$

Solving the above linear system gives the weighting coefficients as

$$a_{-1}^{(1)} = \frac{q_0}{c^m - (c^2 + 4h^2)^{m/2}}, \quad a_0 = 0, \quad a_1^{(1)} = -\frac{q_0}{c^m - (c^2 + 4h^2)^{m/2}}.$$

https://doi.org/10.1017/S1446181121000237 Published online by Cambridge University Press

For finding the weighting coefficients for the second derivative, let

$$q_1 = \frac{m(c^2 + (m-1)h^2)(c^2 + h^2)^{m/2}}{(c^2 + h^2)^2}.$$

The weighting coefficients are solutions of the linear system

$$\begin{pmatrix} w_0 & w_1 & w_2 \\ w_1 & w_0 & w_1 \\ w_2 & w_1 & w_0 \end{pmatrix} \begin{pmatrix} a_{-1}^{(2)} \\ a_0^{(2)} \\ a_1^{(2)} \end{pmatrix} = \begin{pmatrix} q_1 \\ mc^{m-2} \\ q_1 \end{pmatrix}.$$

Solving the above linear system gives

$$a_{-1}^{(2)} = a_1^{(2)} = \frac{-mc^{m-2}h^2(c^2 + h^2)^{m/2-2}(h^2 - (m-3)c^2)}{c^m(c^m + (c^2 + 4h^2)^{m/2}) - 2(c^2 + h^2)^m}$$

and

$$a_0^{(2)} = \frac{m}{c^2}\left(1 + \frac{2h^2(c^2 + h^2)^{m-2}(h^2 - (m-3)c^2)}{c^m(c^m + (c^2 + 4h^2)^{m/2}) - 2(c^2 + h^2)^m}\right).$$

In the limit when the shape parameter c is much larger than the grid size h, that is, $c \gg h$, it can be shown that

$$a_1^{(1)} = \frac{1}{2h}\left(1 + \left(1 - \frac{m}{2}\right)\frac{h^2}{c^2} - \frac{m^2 - 30m + 56}{24}\frac{h^4}{c^4}\right),$$

$$a_1^{(2)} = \frac{1}{h^2}\left(1 - \frac{(m-2)(m-5)}{2(m-3)}\frac{h^2}{c^2} + \frac{(m-2)(m^3 + 8m^2 - 111m + 282)}{24(m-3)^2}\frac{h^4}{c^4}\right)$$

and

$$a_0^{(2)} = -\frac{2}{h^2}\left(1 - \frac{(m-5)(m-2)}{2(m-3)}\frac{h^2}{c^2} - \frac{(m-2)(m^3 - 19m^2 + 87m - 141)}{12(m-3)^2}\frac{h^4}{c^4}\right).$$

The formulas presented in this work are new and these recover the special cases of RBF-FDs for multiquadrics [1] and inverse multiquadrics [26].

4. Development of RBF-FD method for SABR PDE

This section develops the numerical method for the solution of the SABR PDE (2.2) using the RBF-FD approximations derived in the previous section. For the pricing of options under the Heston model, there exist a few alternating direction implicit (ADI) schemes [13, 18, 36]. Although it is possible to develop an ADI-RBF-FD method in a similar way, a different approach is developed in this work.

https://doi.org/10.1017/S1446181121000237 Published online by Cambridge University Press

Assume that $\beta > 0$ and $F \geq 0$. Using the substitution $\tau = T - t$, the pricing equation (2.2) becomes

$$\frac{\partial V}{\partial \tau} = \frac{1}{2}\alpha^2 F^{2\beta}\frac{\partial^2 V}{\partial F^2} + \rho\nu\alpha^2 F^{\beta}\frac{\partial^2 V}{\partial F \partial \alpha} + \frac{1}{2}\nu^2\alpha^2\frac{\partial^2 V}{\partial \alpha^2}, \quad (F, \alpha, \tau) \in \mathbb{R}^+ \times \mathbb{R}^+ \times [0, T] \tag{4.1}$$

with initial condition $V(F, \alpha, 0) = \phi(F, \alpha)$ and absorbing boundary condition $V(0, \alpha, \tau) = 0$.

The pricing equation (4.1) is defined on an unbounded domain. For development of the RBF-FD method, the problem is localized to a finite domain $[0, F_{\max}] \times [0, \alpha_{\max}] \times [0, T]$. Localizing the problem requires that additional boundary conditions be imposed. For a call option, these conditions are given by Kienitz et al. [20] as

$$\frac{\partial V}{\partial F}(F_{\max}, \alpha, \tau) = 1, \quad \frac{\partial V}{\partial \tau}(F, 0, \tau) = 0$$

and

$$\frac{\partial V}{\partial \tau}(F, \alpha_{\max}, \tau) = \frac{1}{2}\alpha_{\max}^2 F^{2\beta}\frac{\partial^2 V}{\partial F^2}(F, \alpha_{\max}, \tau). \tag{4.2}$$

For a put option, the additional boundary conditions are

$$\frac{\partial V}{\partial F}(F_{\max}, \alpha, \tau) = 0, \quad \frac{\partial V}{\partial \tau}(F, 0, \tau) = 0$$

and

$$\frac{\partial V}{\partial \tau}(F, \alpha_{\max}, \tau) = \frac{1}{2}\alpha_{\max}^2 F^{2\beta}\frac{\partial^2 V}{\partial F^2}(F, \alpha_{\max}, \tau).$$

Consider uniformly spaced grid nodes in the F- and α-directions with spacings $h_F = F_{\max}/M$ and $h_\alpha = \alpha_{\max}/J$, respectively. Denote grid nodes in the (F, α)-space by (F_i, α_j), where $F_i = ih_F, 0 \leq i \leq M$ and $\alpha_j = jh_\alpha$ for $0 \leq j \leq J$.

Let $V_{ij}(\tau)$ denote the option price at the node (F_i, α_j, τ) and consider the following RBF-FD approximations:

$$D_{FF}V_{ij}(\tau) \approx \frac{\partial^2 V}{\partial F^2}(F_i, \alpha_j, \tau), \quad D_{\alpha\alpha}V_{ij}(\tau) \approx \frac{\partial^2 V}{\partial \alpha^2}(F_i, \alpha_j, \tau)$$

given by

$$\begin{aligned} D_{FF}V_{ij}(\tau) &= a_{-1,F}^{(2)}V_{i-1,j}(\tau) + a_{0,F}^{(2)}V_{ij}(\tau) + a_{1,F}^{(2)}V_{i+1,j}(\tau), \\ D_{\alpha\alpha}V_{ij}(\tau) &= a_{-1,\alpha}^{(2)}V_{i,j-1}(\tau) + a_{0,\alpha}^{(2)}V_{ij}(\tau) + a_{1,\alpha}^{(2)}V_{i,j+1}(\tau). \end{aligned}$$

The algorithm development is presented for multiquadrics (MQ), which corresponds to the case $m = 1$ in (3.1). For $c \gg h_F$, retaining only terms in h_F^2/c^2, the weighting

https://doi.org/10.1017/S1446181121000237 Published online by Cambridge University Press

coefficients $a_{i,F}^{(2)}$ for $-1 \le i \le 1$ are given by

$$a_{i,F}^{(2)} = \frac{1}{h_F^2}\Big(1 + \frac{h_F^2}{c^2}\Big), \quad i = -1,\ 1, \quad a_{0,F}^{(2)} = -\frac{2}{h_F^2}\Big(1 + \frac{h_F^2}{c^2}\Big).$$

The coefficients $a_{i,\alpha}^{(2)}$, $-1 \le i \le 1$, are given by similar expressions. Since the SABR PDE does not contain any convection term, no upwinding discretizations need to be employed as for the Heston PDE where the presence of convection terms due to the drift terms in the asset and volatility dynamics may lead to oscillations in the numerical solutions when convection is dominant.

The RBF-FD approximation $D_{F\alpha}V_{ij}(\tau)$ for the cross-derivative term $(\partial^2 V/\partial F\partial\alpha)$ (F_i, α_j, τ) is given as

$$D_{F\alpha}V_{ij}(\tau) = a_{12}(V_{i+1,j+1}(\tau) - V_{i-1,j+1}(\tau) - V_{i+1,j-1}(\tau) + V_{i-1,j-1}(\tau)),$$

where

$$a_{12} = \frac{1}{4h_F h_\alpha}\Big(1 + \frac{3h_F^2}{2c^2} + \frac{3h_\alpha^2}{2c^2} - \frac{9h_F^2 h_\alpha^2}{4c^4}\Big).$$

This discretization of the cross-derivative term leads to a nine-point computational stencil at an interior point of the computational domain. Other possibilities leading to seven-point computational stencils are given by Thakoor et al. [30].

Let $\hat{a}_{ij} = \alpha_j^2 F_i^{2\beta}/2$, $\hat{b}_{ij} = \rho\nu\alpha_j^2 F_i^{\beta}$ and $\hat{c}_j = \nu^2\alpha_j^2/2$. Then, at the interior grid points (F_i, α_j) of the (F, α)-computational domain, the discretization of (4.1) is given by

$$V_{ij}'(\tau) = \hat{a}_{ij}D_{FF}V_{ij}(\tau) + \hat{b}_{ij}D_{F\alpha}V_{ij}(\tau) + \hat{c}_j D_{\alpha\alpha}V_{ij}(\tau), \quad 1 \le i \le M-1, \quad 1 \le j \le J-1. \tag{4.3}$$

Consider the vector $\mathbf{U}(\tau) \in \mathbf{R}^{(M-1)(J-1)}$ of call prices at time level τ given by

$$\mathbf{U}(\tau) = [\mathbf{V}_1(\tau),\ \mathbf{V}_2(\tau), \ldots, \mathbf{V}_{J-1}(\tau)]^T,$$

where

$$\mathbf{V}_j(\tau) = [V_{1j}(\tau),\ V_{2j}(\tau), \ldots, V_{M-1,j}(\tau)]^T, \quad 0 \le j \le J.$$

For $1 \le i \le M-1$ and $1 \le j \le J-1$, denote

$$\begin{aligned}
\hat{d}_{i-1,j} &= \hat{a}_{ij}a_{-1,F}^{(2)}, & \hat{d}_{ij} &= \hat{a}_{ij}a_{0,F}^{(2)} + \hat{c}_j a_{0,\alpha}^{(2)}, & \hat{d}_{i+1,j} &= \hat{a}_{ij}a_{1,F}^{(2)},\\
\hat{d}_{i-1,j-1} &= \hat{b}_{ij}a_{12}, & \hat{d}_{i,j-1} &= \hat{c}_j a_{-1,\alpha}^{(2)}, & \hat{d}_{i+1,j-1} &= -\hat{b}_{ij}a_{12},\\
\hat{d}_{i-1,j+1} &= -\hat{b}_{ij}a_{12}, & \hat{d}_{i,j+1} &= a_{1,\alpha}^{(2)}\hat{c}_j, & \hat{d}_{i+1,j+1} &= \hat{b}_{ij}a_{12}.
\end{aligned}$$

https://doi.org/10.1017/S1446181121000237 Published online by Cambridge University Press

For $1 \le j \le J-1$, consider the tridiagonal matrices A_{1j}, A_{2j} and A_{3j} in $\mathbb{R}^{(M-1)\times(M-1)}$ given by

$$A_{1j} = \begin{pmatrix} \hat{d}_{1,j-1} & \hat{d}_{2,j-1} & & & \\ \hat{d}_{1,j-1} & \hat{d}_{2,j-1} & \hat{d}_{3,j-1} & & \\ & \ddots & \ddots & \ddots & \\ & & \hat{d}_{M-3,j-1} & \hat{d}_{M-2,j-1} & \hat{d}_{M-1,j-1} \\ & & & \hat{d}_{M-2,j-1} & \hat{d}_{M-1,j-1} \end{pmatrix},$$

$$A_{2j} = \begin{pmatrix} \hat{d}_{1j} & \hat{d}_{2j} & & & \\ \hat{d}_{1j} & \hat{d}_{2,j} & \hat{d}_{3,j} & & \\ & \ddots & \ddots & \ddots & \\ & & \hat{d}_{M-3,j} & \hat{d}_{M-2,j} & \hat{d}_{M-1,j} \\ & & & \hat{d}_{M-2,j} & \hat{d}_{M-1,j} \end{pmatrix}$$

and

$$A_{3j} = \begin{pmatrix} \hat{d}_{1,j+1} & \hat{d}_{2,j+1} & & & \\ \hat{d}_{1,j+1} & \hat{d}_{2,j+1} & \hat{d}_{3,j+1} & & \\ & \ddots & \ddots & \ddots & \\ & & \hat{d}_{M-3,j+1} & \hat{d}_{M-2,j+1} & \hat{d}_{M-1,j+1} \\ & & & \hat{d}_{M-2,j+1} & \hat{d}_{M-1,j+1} \end{pmatrix}.$$

Let the block-tridiagonal matrix $\mathbf{A} \in \mathbb{R}^{(M-1)(J-1)\times(M-1)(J-1)}$ be given by

$$\mathbf{A} = \begin{pmatrix} A_{21} & A_{31} & & & \\ A_{12} & A_{22} & A_{32} & & \\ & \ddots & \ddots & \ddots & \\ & & A_{1,J-2} & A_{2,J-2} & A_{3,J-2} \\ & & & A_{1,J-1} & A_{2,J-1} \end{pmatrix}.$$

Not accounting for the Neumann boundary conditions (4.2) (we show later in this work how these are incorporated to obtain the full set of ordinary differential equations), we obtain the initial value problem given by

$$\mathbf{U}'(\tau) = \mathbf{A}\mathbf{U}(\tau) + \bar{\mathbf{b}}(\tau), \quad 0 \le \tau \le T \tag{4.4}$$

with initial condition $\mathbf{U}(0) = [\mathbf{u}_1, \mathbf{u}_2, \ldots, \mathbf{u}_{J-1}]^T$, where $\mathbf{u}_i = (F_i - K)^+\bar{\mathbf{1}}$ and $\bar{\mathbf{1}} \in \mathbb{R}^{M-1}$ is a vector of ones. The vector

$$\bar{\mathbf{b}}(\tau) = [\tilde{\mathbf{b}}_1(\tau), \tilde{\mathbf{b}}_2(\tau), \ldots, \tilde{\mathbf{b}}_{J-1}(\tau)]^T$$

consists of option values not in the vector $\mathbf{U}(\tau)$. The vector $\tilde{\mathbf{b}}_j$ is given by

$$\tilde{\mathbf{b}}_j(\tau) = [\tilde{b}_{1j}(\tau), \tilde{b}_{2j}(\tau), \ldots, \tilde{b}_{M-1,j}]^T, \quad 1 \le j \le J-1,$$

https://doi.org/10.1017/S1446181121000237 Published online by Cambridge University Press

where its components are

$$\begin{aligned}\tilde{b}_{11}(\tau) &= \hat{d}_{00}V_{00}(\tau) + \hat{d}_{10}V_{10}(\tau) + \hat{d}_{20}V_{20}(\tau) + \hat{d}_{01}V_{01}(\tau) + \hat{d}_{02}V_{02}(\tau),\\ \tilde{b}_{i1} &= \hat{d}_{i,0}V_{i,0}(\tau) + \hat{d}_{i+1,0}V_{i+1,0}(\tau) + \hat{d}_{i+2,0}V_{i+2,0}(\tau), \quad 2 \le i \le M-2,\\ \tilde{b}_{M-1,1} &= \hat{d}_{M-2,0}V_{M-2,0}(\tau) + \hat{d}_{M-1,0}V_{M-1,0}(\tau) + \hat{d}_{M,0}V_{M,0}(\tau) + \hat{d}_{M,1}V_{M,1}(\tau) + \hat{d}_{M,2}V_{M,2}(\tau).\end{aligned}$$

For $2 \le j \le J-2$, the vectors $\tilde{\mathbf{b}}_j(\tau) \in \mathbb{R}^{M-1}$ have entries

$$\begin{aligned}\tilde{b}_{1j}(\tau) &= \hat{d}_{0,j-1}V_{0,j-1}(\tau) + \hat{d}_{0,j}V_{0,j}(\tau) + \hat{d}_{0,j+1}V_{0,j+1}(\tau),\\ \tilde{b}_{ij}(\tau) &= 0, \quad 2 \le i \le M-2,\\ \tilde{b}_{M-1,j}(\tau) &= \hat{d}_{M,j-1}V_{M,j-1}(\tau) + \hat{d}_{M,j}V_{0,j}(\tau) + \hat{d}_{M,j+1}V_{0,j+1}(\tau)\end{aligned}$$

and the entries of the vector $\tilde{\mathbf{b}}_{J-1} \in \mathbb{R}^{M-1}$ are given by

$$\begin{aligned}\tilde{b}_{1,J-1}(\tau) &= \hat{d}_{0,J-2}V_{0,J-2}(\tau) + \hat{d}_{0,J-1}V_{0,J-1}(\tau) + \hat{d}_{0,J}V_{0,J}(\tau) + \hat{d}_{1,J}V_{1,J}(\tau) + \hat{d}_{2,J}V_{2,J}(\tau),\\ \tilde{b}_{i,J-1}(\tau) &= \hat{d}_{i-1,J}V_{i-1,J}(\tau) + \hat{d}_{i,J}V_{i,J}(\tau) + \hat{d}_{i+1,J}V_{i+1,J}(\tau), \quad 2 \le i \le M-2\end{aligned}$$

and

$$\begin{aligned}\tilde{b}_{M-1,J-1}(\tau) = \hat{d}_{M-2,J}V_{M-2,J}(\tau) &+ \hat{d}_{M-1,J}V_{M-1,J}(\tau) + \hat{d}_{M,J-1}V_{M,J-2}(\tau)\\ &+ \hat{d}_{M,J-1}V_{M,J-1}(\tau) + \hat{d}_{M,J}V_{M,J}(\tau).\end{aligned}$$

The following shows how to obtain the full linear system of ordinary differential equations for time stepping. First, since the boundary condition $V(0, \alpha, \tau) = 0$, we have $V_{0,j}(\tau) = 0$ for $0 \le j \le J$. The other boundary conditions which are of Neumann type are accounted for in the following way. The condition $(\partial V/\partial\tau)(F, 0, \tau) = 0$ means that $V_{i,0}(\tau) = 0$ for $0 \le i \le M$. At the boundary $F = F_{\max}$, the boundary condition $(\partial V/\partial F)(F_{\max}, \alpha, \tau) = 1$ is discretized by a left-sided derivative $D_F^- V_{M,j} = 1, 1 \le j \le J-1$, where

$$D_F^- V_{M,j}(\tau) = \frac{1}{2h_F}\Big(1 - \frac{h_F^2}{c^2}\Big)[V_{M-2,j}(\tau) - 4V_{M-1,j}(\tau) + 3V_{M,j}(\tau)].$$

Then, on the boundary $F = F_{\max}$,

$$V_{M,j}(\tau) = \frac{1}{3}\Big(\frac{2h_F}{1 - h_F^2/c^2} - V_{M-2,J}(\tau) + 4V_{M-1,J}(\tau)\Big). \tag{4.5}$$

At $\alpha = \alpha_{\max}$, the condition (4.2) is discretized as

$$V'_{i,J}(\tau) = \hat{a}_{i,J}D_{FF}V_{i,J}(\tau), \quad 1 \le i \le M-1.$$

Then

$$V'_{i,J}(\tau) = \hat{d}_{i-1,J}V_{i-1,J}(\tau) + \hat{a}_{i,J}a^{(2)}_{0,F}V_{i,J}(\tau) + \hat{d}_{i+1,J}V_{i+1,J}(\tau), \quad 1 \le i \le M-1. \tag{4.6}$$

Augmenting $\mathbf{U}(\tau)$ by the vector of option values when $\alpha = \alpha_{\max}$ and denoting

$$\hat{\mathbf{U}}(\tau) = [\mathbf{V}_1(\tau), \mathbf{V}_2(\tau), \ldots, \mathbf{V}_J(\tau)],$$

https://doi.org/10.1017/S1446181121000237 Published online by Cambridge University Press

we obtain the full system of differential equations

$$\hat{\mathbf{U}}'(\tau) = \hat{\mathbf{A}}\hat{\mathbf{U}}(\tau) + \hat{\mathbf{b}}(\tau), \tag{4.7}$$

where $\hat{\mathbf{A}} \in \mathbb{R}^{(M-1)J\times(M-1)J}$ and $\hat{\mathbf{b}}(\tau) \in \mathbb{R}^{(M-1)J}$ are modifications brought to the matrix $\mathbf{A}$ and vector $\bar{\mathbf{b}}(\tau)$ in (4.4) to account for the boundary conditions at $F = F_{\max}$ and $\alpha = \alpha_{\max}$ given by (4.5) and (4.6), respectively.

4.1. Time-integration scheme There are different possibilities for the time integration of (4.7). A one-step exponential time integration [23] would require the computation of an exponential matrix. This can be efficiently carried out via the Carathéodory–Fejer approximation and contour integrals [25]. For simplicity, an implicit Euler time stepping is described below. Using N time steps in $[0, T]$, let $k = T/N$ denote the step size with time nodes $\tau_n = nk$, $0 \le n \le N$. Let $\hat{\mathbf{U}}^n = [\mathbf{V}_1(\tau_n), \mathbf{V_2}(\tau_n), \ldots, \mathbf{V}_J(\tau_n)]^T$ and $\hat{\mathbf{b}}^n = \hat{\mathbf{b}}(\tau_n)$. An implicit Euler discretization of (4.7) gives the time-stepping procedure

$$(I - k\hat{\mathbf{A}})\hat{\mathbf{U}}^{n+1} = \hat{\mathbf{U}}^n + k\hat{\mathbf{b}}^{n+1}, \quad 0 \le n \le N-1,$$

with initial condition $\hat{\mathbf{U}}^0$ determined by the payoff function as previously described.

4.2. Numerical stability Problem (4.1) is a two-dimensional diffusion equation with a mixed derivative term. For multidimensional problems, but with constant coefficients and periodic boundary conditions, in't Hout and Welfert [19] have presented a stability analysis for second-order ADI schemes. The numerical method in this work uses an implicit Euler time stepping, but variable coefficients and nonperiodic boundary conditions for the problem considered here will bring difficulties in a matrix method for carrying out the stability analysis.

Another approach for the stability analysis would be to use the principle of frozen coefficient problems. Von Neumann analyses [5] can then be carried out for constant-coefficient problems which are obtained by fixing the coefficients at their values at each point in the computational domain [22, 28]. The variable-coefficient problem is stable if each frozen coefficient problem is stable. This would require finding the amplification factor for the fully discrete scheme.

The implicit Euler discretization of (4.3) can be written as

$$V_{ij}^{n+1} = V_{ij}^n + k\hat{a}_{ij}D_{FF}V_{ij}^{n+1} + k\hat{b}_{ij}D_{F\alpha}V_{ij}^{n+1} + k\hat{c}_jD_{\alpha\alpha}V_{ij}^{n+1}, \quad n \ge 0. \tag{4.8}$$

Let

$$V_{ij}^n = g^n(\xi_1 h_F, \xi_2 h_\alpha)e^{\imath(i\xi h_F + j\xi_2 h_\alpha)}, \tag{4.9}$$

where $\imath$ is the unit imaginary complex number, ξ_1 and ξ_2 are wave numbers and $g(\xi_1 h_F, \xi_2 h_\alpha)$ is the amplification factor. The stability condition would require that

https://doi.org/10.1017/S1446181121000237 Published online by Cambridge University Press

the amplification factor satisfies $|g(\xi_1 h_F, \xi_2 h_\alpha)| \le 1$. Substituting (4.9) in (4.8),

$$g(\xi_1 h_F, \xi_2 h_\alpha) = \Bigg(1 + 4\hat{a}_{ij}\gamma_F \sin^2 \frac{\xi_1 h_F}{2} + 4\hat{b}_{ij}\gamma_{F\alpha} \sin \xi_1 h_F \sin \xi_2 h_\alpha + 4\hat{c}_j \gamma_\alpha \sin^2 \frac{\xi_2 h_\alpha}{2}\Bigg)^{-1}, \tag{4.10}$$

where

$$\gamma_F = \frac{k}{h_F^2}\Big(1 + \frac{h_F^2}{c^2}\Big), \quad \gamma_\alpha = \frac{k}{h_\alpha^2}\Big(1 + \frac{h_\alpha^2}{c^2}\Big), \quad \gamma_{F\alpha} = \frac{k}{4h_\alpha h_F}\Big(1 + \frac{3h_F^2}{2c^2} + \frac{3h_\alpha^2}{2c^2} - \frac{9h_F^2 h_\alpha^2}{4c^4}\Big).$$

We assume that $\beta > 0$ and $F \ge 0$. Since $\hat{a}_{ij} = \alpha_j^2 F_i^{2\beta}/2$ and $\hat{c}_j = \nu^2 \alpha_j^2/2$, we find that both $\hat{a}_{ij}$ and $\hat{c}_j$ are nonnegative. When the correlation coefficient $\rho > 0$, the coefficient $\hat{b}_{ij} = \rho\nu\alpha_j^2 F_i^\beta$ is also nonnegative. Therefore, for a positive correlation coefficient ρ, the amplification factor (4.10) satisfies the stability condition $|g(\xi_1 h_F, \xi_2 h_\alpha)| \le 1$.

When the correlation $\rho < 0$, establishing that $|g(\xi_1 h_F, \xi_2 h_\alpha)| \le 1$ is not straightforward. In this case, in order to validate the stability of the numerical scheme, an experimental study is described in the next section. The results show that the errors in the numerical solution remain small with larger time steps. Numerical investigation of the magnitude of the amplification factor for different parabolic mesh ratios also did not reveal any violation of the inequality $|g(\xi_1 h_F, \xi_2 h_\alpha)| \le 1$.

5. Numerical results

In this section, some numerical examples are considered to illustrate the performance of the proposed scheme in achieving arbitrage-free and accurate prices. All numerical experiments have been performed using Matlab R2017a on a Core i5 laptop with 16 GB RAM and speed 3.60 GHz. In all the numerical experiments, we choose $F_{\max} = 4E$ and $\alpha_{\max} = 4\hat{\alpha}$ unless stated otherwise.

5.1. No-arbitrage pricing The first numerical example draws a comparison of computed implied volatilities obtained using the RBF-FD method, the no-arbitrage closed-form (No-Arb CF) approximation method [33] and the standard approximation (Std SABR) [16] to demonstrate that the proposed method is arbitrage-free. Figure 1 shows the implied volatility curve for a low-maturity problem with $T = 1$. The other parameters are given by an initial volatility of $\hat{\alpha} = 0.1$, a CEV elasticity of $\beta = 0.1$, with zero correlation $\rho = 0$, a volatility-of-volatility (vol-vol) of $\nu = 0.1$ and the initial forward price is chosen as $f = 0.05$ [33]. The results are benchmarked with a Monte Carlo (MC) simulation technique with 100 000 time steps. Note that the implied volatilities computed using the no-arbitrage closed-form approximation method and the RBF-FD method agree closely with those computed using the MC simulation method, while the computed implied volatilities of the standard SABR model [16] deviate from the MC results for low strikes. Yang et al. [33] mentioned that their approximations work well when the total vol-vol ($\nu\sqrt{T}$) parameter is small, but, as

https://doi.org/10.1017/S1446181121000237 Published online by Cambridge University Press

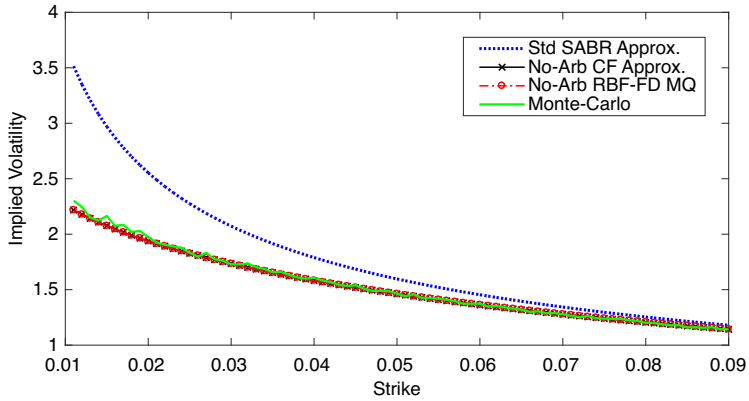

FIGURE 1. Implied volatility for low-strikes problem (colour available online).

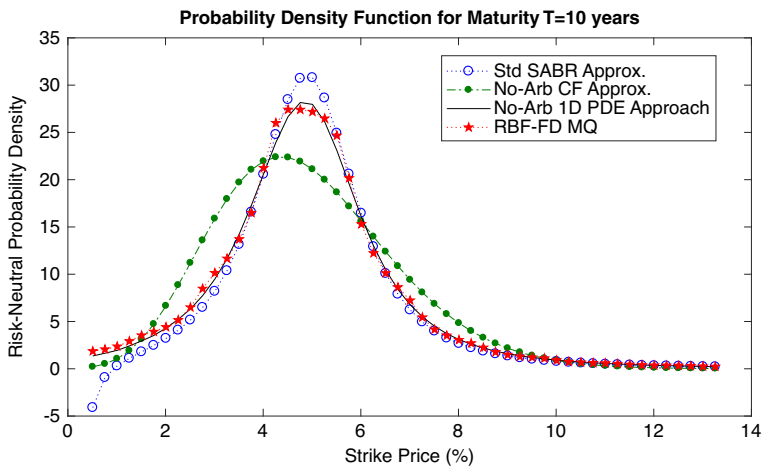

FIGURE 2. Positive probability density using the RBF-FD MQ method.

T becomes large, the formula leads to biased results. We therefore consider a longer maturity problem in the next example.

Doust [10] showed that the implied volatility approximation [16] can result in a negative probability density function for long-dated options. Using the same set of parameters, $f = 0.0488$ with the model parameters given by $(\hat{\alpha}, \beta, \rho, \nu) = (0.026, 0.5, -0.1, 0.4)$, we give the no-arbitrage density function obtained by the RBF-FD multiquadric (MQ) method in Figure 2 and the RBF-FD inverse multiquadric (IMQ) method, which corresponds to the case $m = -1$ (3.1), in Figure 3. Note that both methods are always positive, whereas that of the standard SABR [16] goes negative for low strikes. Comparison is carried out against the no-arbitrage one-dimensional PDE (No-Arb 1D-PDE) method [17] and the no-arbitrage closed-form (No-Arb CF)

https://doi.org/10.1017/S1446181121000237 Published online by Cambridge University Press

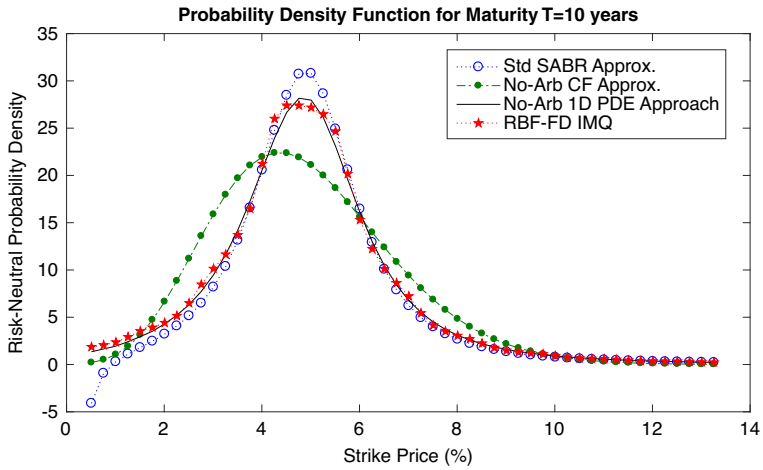

FIGURE 3. Positive probability density using the RBF-FD IMQ method.

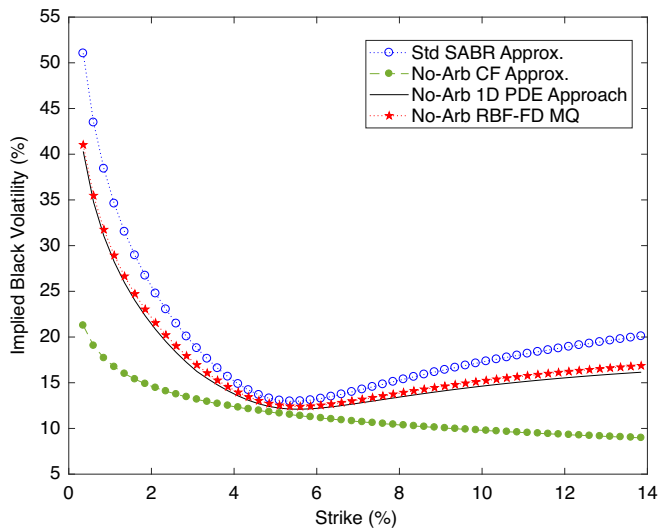

FIGURE 4. Implied volatilities for different strike prices.

approximation by Yang et al. [33]. The corresponding implied volatilities over the range of strike prices $[0, 0.14]$ are given in Figure 4. We observe that while the standard SABR [16] deviates as the strike price decreases, there is a close agreement between the RBF-FD and the No-Arb 1D-PDE methods.

5.2. Option prices: uncorrelated case Table 1 gives the results for pricing a call option with a strike price of $K = 1.1$ and a very short maturity of one month ($T = 1/12$) in the uncorrelated case. The initial forward price is taken as $f = 1.1$. In this setting,

https://doi.org/10.1017/S1446181121000237 Published online by Cambridge University Press

TABLE 1. Uncorrelated case.

$f = 1.1$, $E = 1.1$, $\beta = 0.8$, $\hat{\alpha} = 0.3$, $\nu = 0.4$, $\rho = 0$, $c = 1.5$, $J = 2^3$								
	$T = 1/12$				$T = 5$			
M	Price	Error	Rate	cpu (s)	Price	Error	Rate	cpu (s)
2^4	0.005 10	3.2e-2	–	0.008	0.287 37	5.6e-3	–	0.007
2^5	0.033 92	1.1e-2	1.503	0.041	0.291 66	1.3e-3	2.090	0.016
2^6	0.034 39	2.9e-3	1.976	0.097	0.292 66	3.2e-4	2.043	0.071
2^7	0.036 67	6.1e-4	2.252	0.152	0.292 90	7.7e-5	2.043	0.178
2^8	0.037 16	1.1e-4	2.398	0.761	0.292 96	1.8e-5	2.095	0.802
2^9	0.037 28	4.5e-6	4.688	4.054	0.292 97	3.6e-6	2.348	4.310
Yang et al. [33]	0.037 28				Ref. price ($M = 2^{10}$)			0.292 97
Hagan et al. [16]	0.037 32				Yang et al. [33]			0.283 87
					Hagan et al. [16]			0.30201

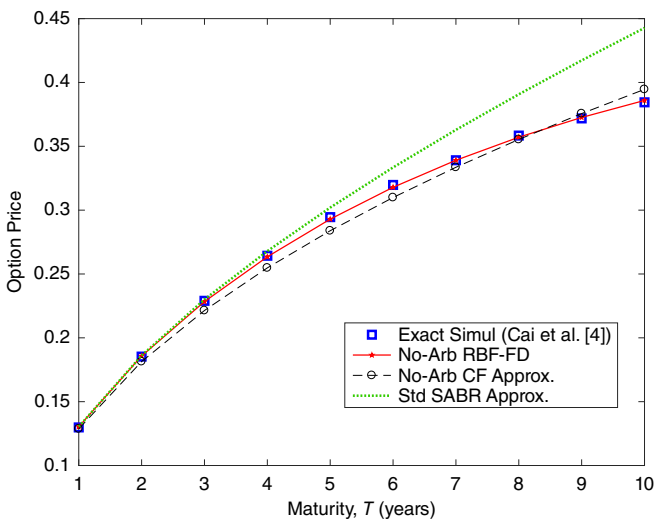

FIGURE 5. Accuracy comparison of the different methods with the exact simulation method when the expansion formula [16] is unreliable.

the expansion formula [16] and the analytical price approximation [33] are expected to be highly accurate, since T, $\hat{\alpha} f^{\beta-1}\nu$ and $\log(K/f)$ are all small. The results indicate that the RBF-FD method is in close agreement with the methods using the expansion formula and the analytical price approximation. For the option with a longer maturity of $T = 5$ years, it can be seen that the numerical method has a smooth second-order

https://doi.org/10.1017/S1446181121000237 Published online by Cambridge University Press

TABLE 2. Comparison of option prices in the correlated case.

$T = 1, f = 0.05, \hat{\alpha} = 0.08, \beta = 0.55, \nu = 0.03, \rho = -0.25, c = 1.5, M = 2^8, J = 2^3$				
E	Analytical approx. [33]	CTMC [9]	RBF-FD	Exact simul. [4]
0.045	0.008 782	0.008 787	0.008 787	0.008 789
0.046	0.008 198	0.008 201	0.008 202	0.008 204
0.047	0.007 640	0.007 642	0.007 642	0.007 644
0.048	0.007 108	0.007 109	0.007 109	0.007 111
0.049	0.006 603	0.006 603	0.006 603	0.006 605
0.050	0.006 124	0.006 122	0.006 122	0.006 124
0.051	0.005 671	0.005 667	0.005 667	0.005 669
0.052	0.005 243	0.005 237	0.005 238	0.005 240
0.053	0.004 839	0.004 833	0.004 833	0.004 835
0.054	0.004 460	0.004 452	0.004 452	0.004 454
0.055	0.004 103	0.004 094	0.004 094	0.004 096

convergence. The reference price comes from computations using a much refined mesh in the F-direction.

The next numerical example tests the accuracy of the RBF-FD scheme for the special case when the expansion formula [16] is not accurate enough. Parameters in the model (2.1) are given by $\rho = 0$, $\beta = 0.8$ and $\nu = 0.4$ and initial forward price and volatility are $f = 1.1$ and $\hat{\alpha} = 0.3$, respectively. The maturity T is allowed to vary in the range $[1, 10]$ for a strike price of $K = 1.1$. The results are benchmarked against the exact simulation method [4]. It is observed that as T increases, the expansion formula of Hagan suffers from an increasing upward bias while the proposed no-arbitrage RBF-FD PDE approach prices coincide with the results of the exact simulation method throughout the range of values of the maturity T.

5.3. Option prices: correlated case Computed RBF-FD prices are reported for the nonzero correlation case with $\rho = -0.25$ in Table 2. Other parameters are the same as those computed using the continuous-time Markov chain (CTMC) approximation [9]. The RBF-FD prices are also compared against the analytical approximation [33] and the exact simulation method [27]. The results demonstrate close agreement of RBF-FD prices with those given by CTMC and the exact simulation methods. Also note that the analytical approximation method [33] yields less accurate prices.

5.4. Optimal shape parameter The selection of the shape parameter in a RBF method plays an important influence on the efficiency and accuracy of the numerical method. An algorithm for selection of the shape parameter based on the leave-one-out cross-validation method was proposed by Rippa [24] and extensions of this approach were described by Fasshauer and Zhang [14]. The choice of the optimal shape

https://doi.org/10.1017/S1446181121000237 Published online by Cambridge University Press

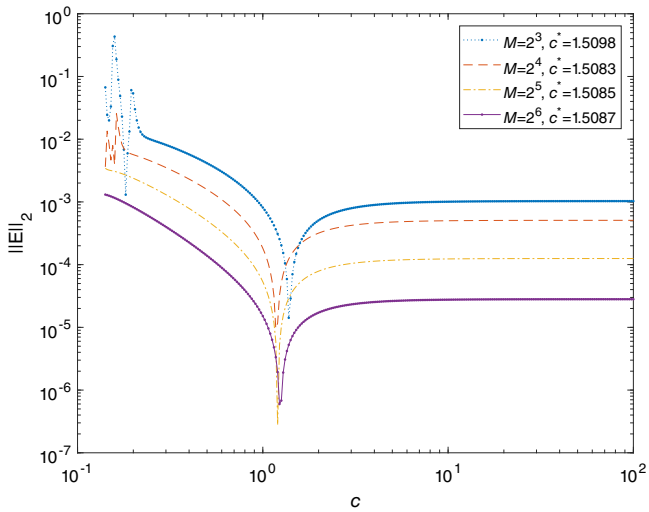

FIGURE 6. Dependence of the ℓ^2 error on the shape parameter c (colour available online).

parameter for PDE problems has been recently considered by Chen et al. [7] and Wang et al. [32]. An algorithm based on minimization of local approximations to the RBF truncation error has been developed by Bayona et al. [2]. However, we believe that adapting this minimization algorithm for determining the optimal shape parameter for the problem considered in this work would require a separate study and we have not pursued it further.

For studying the influence of the shape parameter on the accuracy of the proposed method, we have studied the dependence of the ℓ^2 error on the shape parameter and the results of this experimental study for different values of c are displayed in Figure 6. It is observed that the error decreases until a critical value of $c \approx 1.5$ is reached and, at this approximate value, the error attains a least value. Further increase in c results in a flattening of the ℓ^2 error curve. It is therefore observed that a value of $c = 1.5$ in the numerical method is a good choice.

5.5. Numerical tests for stability A numerical approach for the detection of stability restrictions for option pricing PDEs under stochastic volatility models was employed by Düring and Fournié [12]. A similar approach is used here and the ℓ^2 errors of the numerical solutions are computed for varying values of the parabolic mesh ratios γ_F and γ_α.

European call option prices for the uncorrelated and correlated cases are calculated using the parameters in Table 1 with $T = 0.5$ and in Table 2. The corresponding stability plots for the ℓ^2 error are given in Figures 7(a) and 7(b), respectively. The stability plots are obtained for γ_F varying in the range $[0.2, 0.3, \ldots, 5]$ and a sequence of spatial grid sizes $h_F = [0.02, \ldots, 0.2]$ for the uncorrelated case and

https://doi.org/10.1017/S1446181121000237 Published online by Cambridge University Press

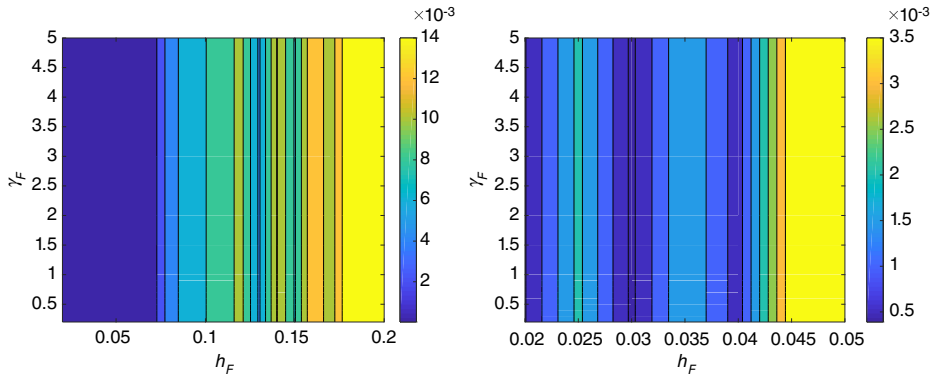

(a) Uncorrelated case. (b) Correlated case.

FIGURE 7. Contour plots for the ℓ^2 error norm against the parabolic mesh ratio γ_F against the spatial mesh h_F in the F-direction.

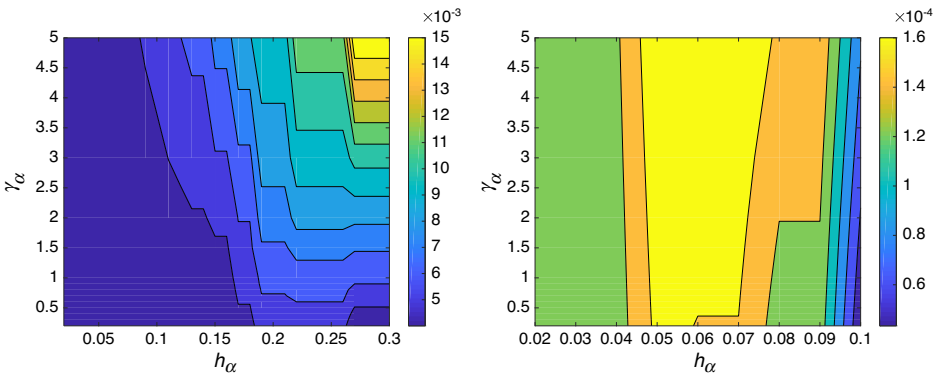

(a) Uncorrelated case. (b) Correlated case.

FIGURE 8. Contour plots for the ℓ^2 error norm against the parabolic mesh ratio γ_α against the spatial mesh h_α in the α-direction.

$h_F = [0.02, \ldots, 0.05]$ for the correlated case. The results displayed in Figures 7–9 show that there is no stability restriction on the time-step size and that accurate numerical solutions are computed in all the cases as evidenced by the small ℓ^2 errors. From Figures 8(a) and 8(b), the same conclusion is reached when the parameter γ_α is varied.

Figures 9(a) and 9(b) show the ℓ^2 error as a function of $(\gamma_F, \gamma_\alpha)$. We observe that the errors remain small and this validates our earlier analysis that the numerical scheme is unconditionally stable.

5.6. Barrier options Yang et al. [34] derived closed-form approximation formulas for pricing continuously monitored down-and-out and up-and-out options. The prices

https://doi.org/10.1017/S1446181121000237 Published online by Cambridge University Press

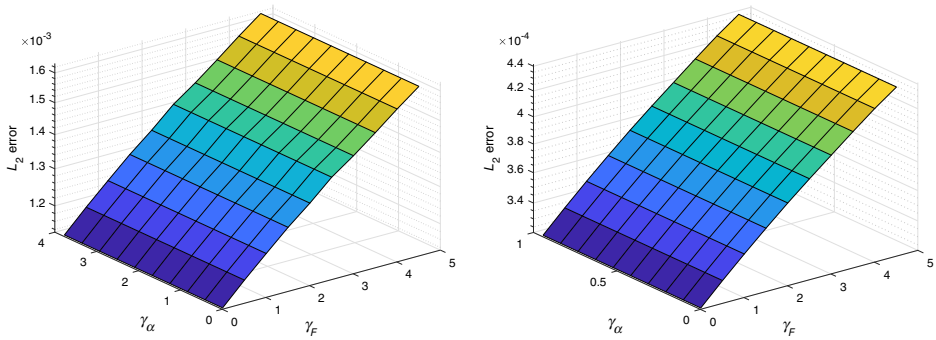

(a) $M = 2^6$ and $J = 2^3$. (b) $M = 2^7$ and $J = 2^3$.

FIGURE 9. Surface plot for the ℓ^2 error against parabolic mesh ratios γ_F and γ_α.

given in their work are used to demonstrate that the proposed RBF-FD method is also an accurate and efficient method for the pricing of barrier options under the SABR dynamics. The parameters in the SABR model are $\beta = 0.5$ and $\nu = 0.1$, the initial forward price is taken as $f = 100$ and the initial volatility is $\hat{\alpha} = 0.1$. A down-and-out call option with strike price $K = 100$ is priced with a lower barrier at $L = 98$ using RBF-FD and the results are given in Table 3. Reference prices are from a MC method via Euler discretization with 1 000 000 simulation samples [34]. The table also shows relative errors (RE) computed using the formula

$$\mathrm{RE} = \frac{|V_{\mathrm{Approx}} - V_{\mathrm{MC}}|}{V_{\mathrm{MC}}}.$$

Table 3 shows that the relative errors are all less than 1% and that the RBF-FD method slightly outperforms the results obtained by the closed-form approximation method in the case of small maturities of $T = 0.5$ and $T = 1$ year.

Figure 10(a) shows that there is a close agreement between the RBF-FD method and the closed-form approximation for $T = 1$. However, for a longer maturity of $T = 5$ years, the authors reported a relative error of 5.0% with MC prices and that the relative error increases as maturity increases. They further mentioned that their formula is not valid for relatively large maturities, since the approximation error is at first order for a positive barrier level. This is illustrated in Figure 10(b), where we observe that as the maturity increases, the closed-form analytical approximation price deviates from the RBF-FD price.

In Table 4, we report the values of double knock-out call options for different values of β with knock-out boundaries at $L = 90$ and $U = 120$. The analytical approximation approach of Yang et al. [34] works only for single-barrier options and the authors mentioned that double-knock-out options must be tackled differently. We therefore do not have any benchmark results for comparison of the RBF-FD computed prices, but,

https://doi.org/10.1017/S1446181121000237 Published online by Cambridge University Press

TABLE 3. Down-and-out call option prices for varying values of ρ.

$f = 100$, $L = 98$, $E = 100$, $\hat{\alpha} = 0.1$, $\beta = 0.5$, $\nu = 0.1$, $F_{\max} = 200$, $\alpha_{\max} = 0.2$						
			Analytical approx. [34]		RBF-FD	
$T = 1/2$	ρ	MC	Price	RE	Price	RE
	–0.1	0.2817	0.2827	0.36%	0.2825	0.28%
	–0.2	0.2820	0.2827	0.24%	0.2825	0.17%
	–0.3	0.2819	0.2827	0.28%	0.2825	0.20%
	–0.4	0.2820	0.2827	0.26%	0.2825	0.16%
	–0.5	0.2813	0.2827	0.50%	0.2824	0.40%
			Analytical approx.		RBF-FD	
$T = 1$	ρ	MC	Price	RE	Price	RE
	–0.1	0.3993	0.4002	0.22%	0.3994	0.01%
	–0.2	0.3996	0.4002	0.15%	0.3993	0.07%
	–0.3	0.3998	0.4002	0.10%	0.3993	0.13%
	–0.4	0.3997	0.4002	0.13%	0.3992	0.11%
	–0.5	0.3995	0.4002	0.17%	0.3992	0.08%

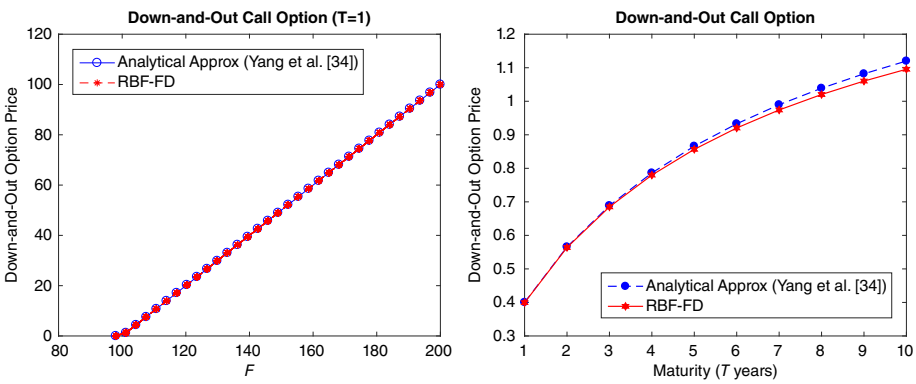

(a) Down-and-out option prices for $T = 1$.

(b) Down-and-out option prices for different values of T.

FIGURE 10. Comparison of down-and-out call options for small- and large-maturity problems.

given the high accuracy of the proposed method for pricing single-knock-out options, it is expected that the results reported here are also highly accurate.

5.7. Randomly scattered nodes We finally consider the pricing of options using the RBF-FD method on scattered nodes by generating Halton points constructed from the Van der Corput sequences [15]. Figure 11 shows the Halton points constructed

https://doi.org/10.1017/S1446181121000237 Published online by Cambridge University Press

TABLE 4. Double knock-out call options prices using the RBF-FD method.

$\hat{\alpha} = 0.2,\ \nu = 0.2,\ \rho = 0.3,\ T = 0.5,\ f = 100,\ M = 2^7, J = 2^5$					
				Price	
L	U	E	$\beta = 0.3$	$\beta = 0.5$	$\beta = 0.7$
90	120	95	5.000 03	5.000 02	5.108 01
90	120	100	0.224 94	0.565 04	1.419 43
90	120	105	0.000 00	0.000 25	0.157 86

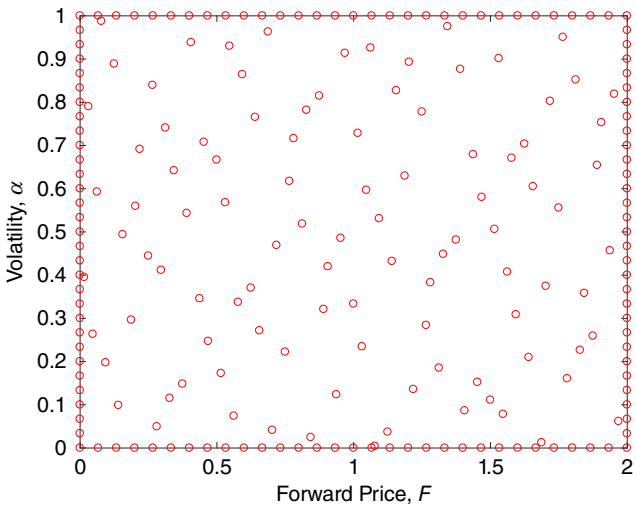

FIGURE 11. Halton grid [15] with $M = 100$ interior points for $F \in [0, 2]$ and $\alpha \in [0, 1]$.

using 100 interior points in a unit square in $\mathbb{R}^2$, and along the boundaries the nodes are partitioned uniformly.

For the parameters $f = 1$, $E = 1$, $\hat{\alpha} = 0.2$, $\beta = 0.5$, $\rho = -0.06$, $\nu = 0.2$ and $T = 0.5$ with $F_{\max} = 2$ and $\alpha_{\max} = 1$, the interpolated option prices on the scattered nodes and the resulting fitted surface are shown in Figure 12.

Finally, a comparison is made between the magnitude of the error norms obtained by the following three methods: a RBF-FD method using randomly scattered grid points, a RBF-FD method on a uniform grid and a standard finite-difference (FD) scheme using central difference approximations. The FD and RBF-FD results are based on the same grid construction. From the results given in Table 5, it is observed that choosing the same range for F for both the FD and RBF-FD schemes gives numerical errors of similar magnitudes. It is also observed that increasing the number of support nodes (ns) for the random grid method leads to more accurate prices.

https://doi.org/10.1017/S1446181121000237 Published online by Cambridge University Press

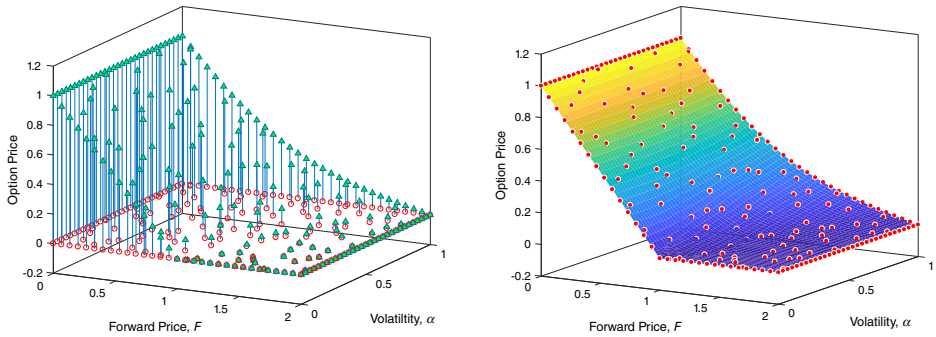

(a) Option prices on scattered nodes (b) Option price fitted surface

FIGURE 12. Option price fitted surface for $F \in [0, 2]$ and $\alpha \in [0, 1]$.

TABLE 5. Option prices obtained on scattered nodes and structured nodes.

$f = 1$, $E = 1$, $\hat{\alpha} = 0.2$, $\beta = 0.5$, $\rho = -0.06$, $\nu = 0.2$, $T = 0.5$, $F_{\max} = 4E$, $\alpha_{\max} = 4\hat{\alpha}$								
				Structured nodes				
Scattered nodes RBF				RBF-FD			FD	
M	ns	Price	RMSE	M	Price	RMSE	Price	RMSE
50	20	0.054 691	1.8e-3	50	0.054 510	2.0e-3	0.054 507	2.0e-3
100	50	0.056 717	2.5e-4	100	0.055 900	5.7e-4	0.055 899	5.7e-4
400	100	0.056 492	2.4e-5	400	0.056 439	3.0e-5	0.056 411	5.7e-5
Analytical approx.		0.056 468						

6. Conclusion

Valuation of options under the popular SABR model using asymptotic implied volatility expansions or analytical approximations using expansions of Bessel operators are unlikely to yield accurate prices for large maturities. Our work addresses this lack of accuracy problem by proposing a novel approach based on the direct numerical solution of the two-dimensional pricing equation with an absorbing boundary condition at zero. The proposed method employed radial basis functions approximations in a finite-difference mode of the spatial derivatives.

New formulas for approximating the first- and second-order derivatives using generalized multiquadrics were derived, and these were shown to recover the approximations for multiquadrics and inverse multiquadrics derived in other studies. The system of ordinary differential equations arising in the computational method was formulated and time integrated using an implicit Euler scheme. Various examples of option pricing problems under SABR were numerically solved. Confirmation of no-arbitrage prices

https://doi.org/10.1017/S1446181121000237 Published online by Cambridge University Press

was established by the validation of nonnegative probability densities computed using multiquadrics and inverse multiquadrics.

Comparisons with existing MC simulation methods showed that accurate European and barrier prices were computed by the new RBF-FD method. One clear advantage of the RBF-FD method over standard finite-difference approaches is that the method can be applied in a meshless approach. Using randomly scattered points in the computational domain, the method was shown to yield accurate prices. As such, the method proposed in this work provides an efficient approach for option pricing under SABR. In a follow-up work, the pricing of American options using the RBF-FD approach will be studied.

Acknowledgements

The author would like to thank the two anonymous reviewers for their valuable suggestions, which have brought significant and important enhancements to this work.

References

[1] V. Bayona, M. Moscoso, M. Carretero and M. Kindelan, "RBF-FD formulas and convergence properties", *J. Comput. Phys.* **229** (2010) 8281–8295; doi:10.1016/j.jcp.2010.07.008.

[2] V. Bayona, M. Moscoso and M. Kindelan, "Optimal variable shape parameter for multiquadric based RBF-FD method", *J. Comput. Phys.* **231** (2012) 2466–2481; doi:10.1016/j.jcp.2011.11.036.

[3] F. Black and M. Scholes, "The pricing of options and other corporate liabilities", *J. Polit. Econ.* **81** (1973) 637–654; http://www.jstor.org/stable/1831029.

[4] N. Cai, Y. Song and N. Chen, "Exact simulation of the SABR model", *Oper. Res.* **65** (2017) 931–951; doi:10.1287/opre.2017.1617.

[5] J. G. Charney, R. Fjørtoft and J. Von Neumann, "Numerical integration of the barotropic vorticity equation", *Tellus* **2** (1950) 237–254; doi:10.3402/tellusa.v2i4.8607.

[6] N. Chen and N. Yang, "The principle of not feeling the boundary for the SABR model", *Quant. Finance* **19** (2019) 427–436; doi:10.1080/14697688.2018.1486037.

[7] W. Chen, Y. Hong and J. Lin, "The sample solution approach for the determination of the optimal shape parameter in the multiquadric function of the Kansa method", *Comput. Math. Appl.* **75** (2018) 2942–2954; doi:10.1016/j.camwa.2018.01.023.

[8] J. Crank and P. Nicolson, "A practical method for numerical evaluation of solutions of partial differential equations of the heat conduction type", *Proc. Cambridge Philos. Soc.* **43** (1947) 50–67; doi:10.1017/S0305004100023197.

[9] Z. Cui, J. L. Kirkby and D. Nguyen, "A general valuation framework for stochastic alpha beta rho and stochastic volatility models", *SIAM. J. Financial Math.* **9** (2018) 520–563; doi:10.1137/1610.1017/S0305004100023197M1106572.

[10] P. Doust, "No-arbitrage SABR", *J. Comput. Finance* **15** (2012) 3–31; doi:10.21314/JCF.2012.254.

[11] B. Dupire, "Pricingwith a smile risk", *Risk* **7** (1994) 18–20; https://www.risk.net/derivatives/equity-derivatives/1500211/pricing-with-a-smile.

[12] B. Düring and M. Fournié, "High-order compact finite difference scheme for option pricing in stochastic volatility models", *J. Comput. Appl. Math.* **236** (2012) 4462–4473; doi:10.1016/j.cam.2012.04.017.

[13] B. Düring and J. Miles, "High-order ADI scheme for option pricing in stochastic volatility models", *J. Comput. Appl. Math.* **316** (2017) 109–121; doi:10.1016/j.cam.2016.09.040.

https://doi.org/10.1017/S1446181121000237 Published online by Cambridge University Press

[14] G. E. Fasshauer and J. G. Zhang, "On choosing optimal shape parameters for the RBF approximation", *Numer. Algorithms* **45** (2007) 345–368; doi:10.1007/s11075-007-9072-8.

[15] G. F. Fasshauer, *Meshfree approximation methods with Matlab*, Volume **6** (World Scientific, Singapore, 2007); doi:10.1142/6437.

[16] P. S. Hagan, D. Kumar, A. S. Lesniewski and D. E. Woodward, "Managing smile risk", *Wilmott Mag.* (2002) 84–108; http://web.math.ku.dk/~rolf/SABR.pdf.

[17] P. S. Hagan, D. Kumar, A. S. Lesniewski and D. E. Woodward, "Arbitrage-free SABR", *Wilmott Mag.* (2014) 60–75; doi:10.1002/wilm.10290.

[18] K. J. in't Hout and S. Foulon, "ADI finite difference schemes for option pricing in the Heston model with correlation", *Int. J. Numer. Anal. Model.* **7** (2010) 303–320; http://global-sci.org/intro/article_detail/ijnam/721.html.

[19] K. J. in't Hout and B.D. Welfert, "Unconditional stability of second-order ADI schemes applied to multidimensional diffusion equations with mixed derivatives", *Appl. Numer. Math.* **59** (2009) 677–692; doi:10.1016/j.apnum.2008.03.016.

[20] J. Kienitz, T. McWalter and R. Sheppard, "PDE methods for SABR", in: *Novel methods in computational finance*, Volume **25** of *Math. Ind.* (Springer, Cham, 2017), pp. 265–291; doi:10.1007/978-3-319-61282-9_15.

[21] F. Le Floc'h and G. Kennedy, "Finite difference techniques for arbitrage-free SABR", *J. Comput. Finance* **20** (2017) 51–79; doi:10.21314/JCF.2016.320.

[22] S. Mishra and M. Svard, "On the stability of numerical schemes via frozen coefficients and the magnetic induction equations", *BIT Numer. Math.* **50** (2009) 85–108; doi:10.1007/s10543-010-0249-5.

[23] N. Rambeerich, D. Y. Tangman, M. R. Lollchund and M. Bhuruth, "High-order computational methods for option valuation under multifactor models", *European J. Oper. Res.* **224** (2013) 219–226; doi:10.1016/j.ejor.2012.07.023.

[24] S. Rippa, "An algorithm for selecting a good value for the parameter c in radial basis function interpolation", *Adv. Comput. Math.* **11** (1999) 193–210; doi:10.1023/A:1018975909870.

[25] T. Schmelzer and L. N. Trefethen, "Evaluating matrix functions for exponential integrators via Carathéodory–Fejér approximation and contour integrals", *Electron. Trans. Numer. Anal.* **29** (2007) 1–18; https://core.ac.uk/download/pdf/1633681.pdf.

[26] F. Soleymani, M. Barfeie and F. K. Haghani, "Inverse multiquadric RBF for computing the weights of FD method: application to American options", *Commun. Nonlinear. Sci. Numer. Simulat.* **64** (2018), 74–88; doi:10.1016/j.cnsns.2018.04.011.

[27] Y. Song, "*Essays on computational methods in financial engineering*", Ph. D. Thesis, Hong Kong University of Science and Technology, 2013; https://doi.org/10.14711/thesis-b1255611.

[28] J. C. Strikwerda, *Finite difference schemes and partial differential equations*, 2nd edn (SIAM, Philadelphia, 2004); https://epubs.siam.org/doi/pdf/10.1137/1.9780898717938.fm.

[29] N. Thakoor, "A non-oscillatory scheme for the one-dimensional SABR model", *Pertanika J. Sci. Technol.* **25** (2017) 1291–1306; http://www.myjurnal.my/filebank/published_article/58141/20.pdf.

[30] N. Thakoor, D. Y. Tangman and M. Bhuruth, "RBF-FD schemes for option valuation under models with price-dependent and stochastic volatility", *Eng. Anal. Bound. Elem.* **92** (2018), 207–217; doi:10.1016/j.enganabound.2017.11.003.

[31] N. Thakoor, D. Y. Tangman and M. Bhuruth, "A spectral approach to pricing of arbitrage-free SABR discrete barrier options", *Comput. Econ.* **54** (2019) 1085–1111; doi:10.1007/s10614-018-9868-8.

[32] F. Wang, W. Chen, C. Zhang and Q. Hua, "Kansa method based on the Hausdorff fractal distance for Hausdorff derivative Poisson equations", *Fractals* **26** (2018) 1850084; doi:10.1142/S0218348X18500846.

[33] N. Yang, N. Chen, Y. Liu and X. Wan, "Approximate arbitrage-free option pricing under the SABR model", *J. Econom. Dynam. Control* **83** (2017) 198–214; doi:10.1016/j.jedc.2017.08.004.

https://doi.org/10.1017/S1446181121000237 Published online by Cambridge University Press

[34] N. Yang, Y. Liu and Z. Cui, "Pricing continuously monitored barrier options under the SABR model: a closed-form approximation", *J. Manag. Sci. Eng.* **2** (2017) 116–131; doi:10.3724/SP.J.1383.202006.

[35] N. Yang and X. Wan, "The survival probability of the SABR model: asymptotics and application", *Quant. Finance* **18** (2018) 1767–1779; doi:10.1080/14697688.2017.1422083.

[36] S. P. Zhu and W. T. Chen, "A predictor–corrector scheme based on ADI method for pricing American puts with stochastic volatility", *Comput. Math. Appl.* **62** (2011) 1–26; doi:10.1016/j.camwa.2011.03.101.

https://doi.org/10.1017/S1446181121000237 Published online by Cambridge University Press